G. Srivalli, B. Raghavarao, M.R.Ch.Sastry / International Journal of Engineering Research and Applications (IJERA) ISSN: 2248-9622 www.ijera.com
Vol. 2, Issue 6, November- December 2012, pp.048-056

Fluid Flow And Heat Transfer Analysis Of Laminar Multiple Square Jets Impinging On A Flat Plate

G. SRIVALLI, B. RAGHAVARAO, M.R.CH.SASTRY
Department of Mechanical Engineering, V.R. Siddhartha Engineering College, Vijayawada.
Department of Mechanical Engineering, V.R. Siddhartha Engineering College, Vijayawada.
Department of Mechanical Engineering, Gudlavalleru Engineering College, Gudlavalleru

Abstract

A computational study is reported on fluid flow and heat transfer from multiple laminar square jets impinging on a flat surface. The parameter which are varied in this study includes fluid Reynolds number (Re=100,300,500), jet to jet spacing (4D,5D,6D) and nozzle exit to plate distance (A_Z) .The commercially available finite volume code Fluent 6.3.26 is used to solve the flow field and heat transfer characteristics. The computationally obtained flow structure reveals the complex interaction of wall jets. Primary peaks are obtained at the stagnation point and secondary peaks are observed at the interaction of the wall jets. Flow structure is strongly affected by the jet -to-plate spacing. A strong correlation between the Nusselt number and pressure distribution is noticed. On the other hand the magnitude of local Nusselt number at the stagnation point is not affected by Jet-to-Jet spacing.

Keywords: Jet impingement, laminar flow, up wash flow, CFD

1. Introduction

Jet impingement flows are frequently used in various industrial equipment for their superior heat and mass transfer characteristics compared to those obtained for the same amount of gas flowing parallel to the target surface. For example, the heat transfer coefficient for the typical application of impinging jets including many heating, cooling, and drying processes is a few times(typically, 2-10 times) higher than that of a cross circulation dryer. Hence, impinging jets are widely used for the drying of continuous sheets of materials such as paper and textiles. Applications of impinging jets also include the manufacture of printed wiring boards, printing processes, production of foodstuffs, deicing of aircraft wings, annealing of metal sheets, tempering of glass, and cooling of the turbine aerofoil. Although there are numerous studies reported in the literature on the subject over the past three decades, impinging jet heat transfer remains an active area of research because of its complicated fluid dynamics. The effects of design variables, such as nozzle geometry and size, nozzle configuration, location of exhaust ports, nozzle-to-impinged surface, and surface motion, and operating variables, such as cross-flow, jet axis velocity on the fluid flow, and heat transfer, need to be characterized in detail for optimal design.

The Jets discharge from round (or) rectangular slots and often bank of such jets are used in the applications. The use of a single circular jet results in a localized high heat transfer rate at the point of jet impingement . Multiple jets produce a more uniform cooling. Nevertheless multiple jets complicate the fluid distribution downstream, where chips require ease of fluid introduction from the smallest volume possible. Most of the effort so far have been developed to the study of circular jets and rectangular jets. The experimental and theoretical investigations on jets are mostly related with turbulent jets. The impingement of confined single and twin turbulent jets though a cross flow was studied by Barata(1). Numerous studies have been reported in the literature on the flow, heat, and mass transfer distributions under single laminar impinging jets (Heiningen(2) , Chou and Hung(3) , Mikhail(4), Yuan(5), Schafer(6) , Wadsworth and Mudawar(7) , and Sezai and Mohamad(8). The effects of interaction between twin planar free-surface jets have been studied experimentally by Slayzak(9) et al. using water as the working fluid. Clayton, D.J., and W. P. Jones, (10) reported Large Eddy Simulation of Impinging Jets in a Confined Flow, Jung-Yang and Mao-De (11) investigated the effect of jet-to-jet spacing on the local Nusselt number for confined circular air jets vertically impinging on a flat plate. The emphasis was placed on the secondary stagnation point associated with the interaction between the opposing wall jets, characterized by an up wash fountain. Although many applications involve turbulent jets, laminar jets also encountered when fluid is highly viscous or the geometry is miniature as in microelectronics. The various factor affecting flow and heat transfer behavior of the impinging laminar square jets have not been systematically investigated. The present work deals with the analysis of laminar, three dimensional, square array of five jets impinging on a isothermal flat surface as shown in fig(1).The broad objectives of the paper are therefore to computationally investigate (i) the flow structure of interacting jets, (ii) the effect of jet - to- jet distance,

jet- to- plate distance and Reynolds number(Re) on flow and heat transfer characteristics.

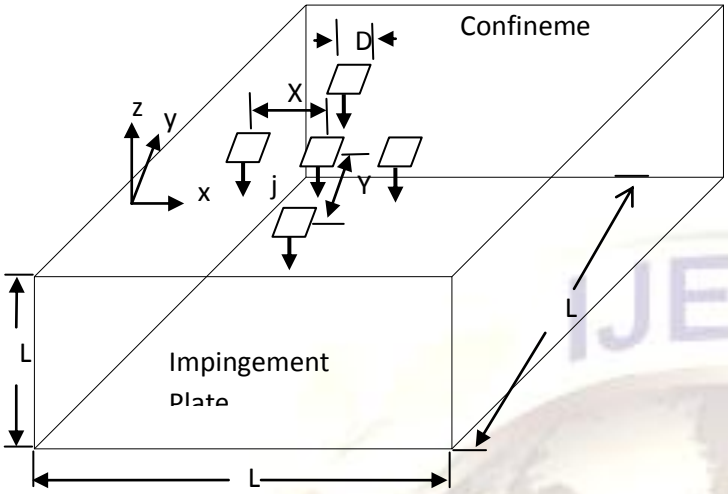

Fig.1 Definitions of geometric parameters and the co-ordinate systems

2. Computation Scheme

The steady state, three-dimensional Navier-Stokes and energy equations for incompressible flows in Cartesian coordinates are used for this study. The buoyancy effect has been neglected..The non dimensional continuity, momentum, and energy equations for laminar flows with constant properties can be written as

$$\frac{\partial U}{\partial X}+\frac{\partial V}{\partial Y}+\frac{\partial W}{\partial Z}=0$$

$$U\frac{\partial U}{\partial X}+V\frac{\partial V}{\partial Y}+W\frac{\partial U}{\partial Z}=-\frac{\partial P}{\partial X}+\frac{1}{Re}\nabla^2 U$$

$$U\frac{\partial V}{\partial X}+V\frac{\partial V}{\partial Y}+W\frac{\partial V}{\partial Z}=-\frac{\partial P}{\partial Y}+\frac{1}{Re}\nabla^2 V$$

$$U\frac{\partial W}{\partial X}+V\frac{\partial W}{\partial Y}+W\frac{\partial W}{\partial Z}=-\frac{\partial P}{\partial Z}+\frac{1}{Re}\nabla^2 W$$

$$U\frac{\partial T}{\partial X}+V\frac{\partial T}{\partial Y}+W\frac{\partial T}{\partial Z}=\frac{1}{RePr}\nabla^2 T$$

Boundary conditions for velocities: the outlet boundary is located far enough downstream for conditions to be substantially developed; accordingly the following conditions are imposed:

$$\frac{\partial U}{\partial X}=\frac{\partial V}{\partial X}=\frac{\partial W}{\partial X}=0 \qquad \text{at } X=0, X=A_X$$

$$\frac{\partial U}{\partial Y}=\frac{\partial V}{\partial Y}=\frac{\partial W}{\partial Y}=0 \qquad \text{at } Y=0, Y=A_Y$$

condition is imposed on the top wall, except at the inlet. Constant pressure outlet condition is applied on all outlet boundaries. Atmospheric pressure and temperature of 300K are applied at the outlets.

3.1 Numerical Solution

All walls are stationary and impervious therefore no slip boundary condition is used for the top and bottom solid walls except the W velocity at the jets exit cross section at the top wall, where it was set to be equal to unity and ,hence, U=V=W=0 at Z=0, Z=A_Z except at nozzle exit, U=V=0,W= -1 at nozzle exit.

Adiabatic boundary conditions are imposed on the top wall, except at the nozzle exit cross section where it was set to be equal to that of ambient. The bottom wall is set to a higher temperature than the ambient.

3. Method of Solution and Validation

A computation mesh suitable for finite volume method is generated using automatic grid generating tool Gambit 2.3.16. The important features of the mesh are (i) structured mesh generated for the entire domain but includes coopered wedge elements where appropriate ,and (ii) fine clustered mesh generated near all the solid walls, at the jet interfaces, and in the up wash flow regions. Grid independent study is carried out for the case of A_Z =1 ,Re 500. When the mesh cell size is increased from 0.18 million to 0.52 million the maximum difference in static pressure distribution along the stagnation line is about 4%. Further increase of mesh size from 0.52 million to 1.43 million , difference in static pressure distribution is about 2%.However,further increase of mesh size from 1.43 million to 1.65 million the difference in average static pressure is less than 1%. In order to reduce the computational cost, 1.43 million mesh is selected as final grid as shown in table 1. Similar grid independent study is done for other cases as well.

MESH SIZE (in millions)	PRESSURE
0.183	0.576
0.526	0.625
1.430	0.656
1.64	0.657

Table:1 MESH

SENSITIVITY

For the purpose of computation five square jets each of 8×8 mm are used, uniform velocity flow condition is imposed at inlet. Ambient air of constant temperature at 300K is specified as the inlet fluid. A constant wall temperature of 400K is applied to the target surface. Adiabatic boundary

A finite volume based solver Fluent 6.3 is used for solving governing equations (continuity, momentum and energy). Flow is considered to be incompressible and constant properties are used because of small variation in temperature and pressure. The solution is considered as converged when the residuals falls below 10^{-4} for momentum,

continuity and 10^{-8} for energy equation . Change in Total surface heat flux for all stagnation point is continuously monitored so that there will be no change in the value for consecutive 300 iterations.

The suitability of numerical scheme, mesh size, accuracy and convergence criterion used in the present study has been validated by comparing the span wise local Nusselt number variation along the length with the available data Sezai, I., Mohamad, A.A., 1991.

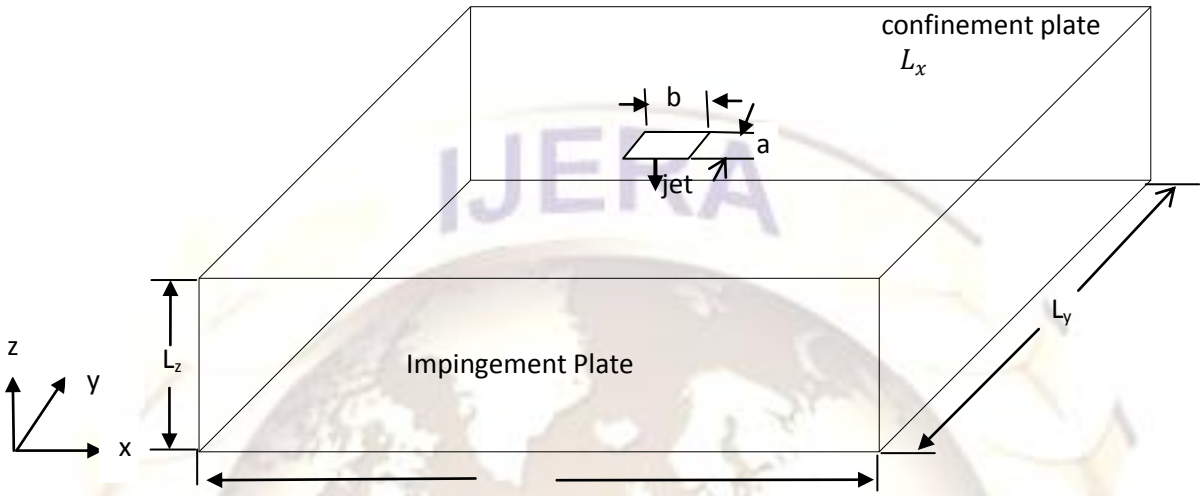

Fig. 2 Boundary conditions for three-dimensional laminar rectangular impingement jet.

The physical domain consists of the semi confinement plate with single rectangular slot of dimension (a×b). When a is nozzle length and b is nozzle width. The aspect ratio is maintained '1' and hence a=b. distance between the impinging plate and top wall is A_Z =2.5 is maintained. Air is used as working fluid, having a prandtl number 0.7 and Reynolds number 300.

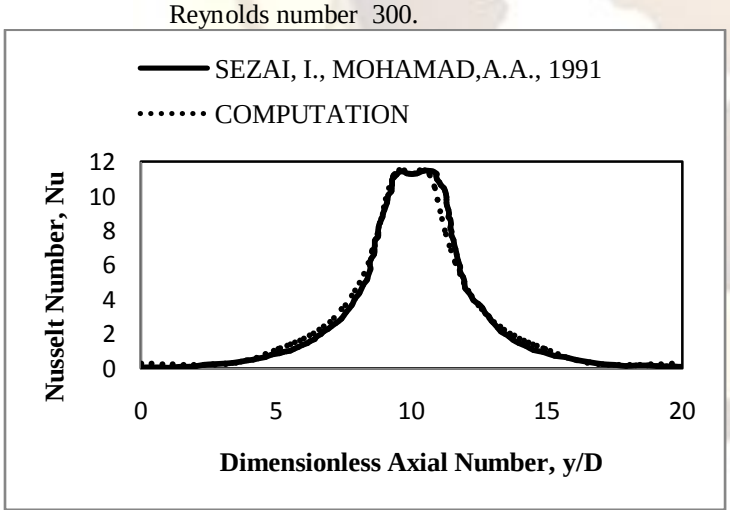

Fig.3 Variation of Nusselt Number for Re=300 at A_Z =2.5 in Y direction

The surface boundary condition analogous to isothermal surface, the agreement between the results obtained by the present methodology and Sezai, I., Mohamad, A.A., 1991 is in good agreement. So, the methodology can be well taken as validated.

3.2 Parameter Investigated

Air is used as the working fluid having a Prandtl number of 0.71. The analysis is performed for the Reynolds number between 100 and 500 and aspect ratios, $A_{Z,}$ between 0.25 and 9.Center-to-centerdistance values between the jets used are 4*D*, 5D and 6*D*, where $X_n = Y_n$ is used for all the cases. The cross section of the nozzles is taken to be square, and the velocity distribution at the exit of the nozzles is assumed to have a flat profile. The parameter investigated in the present study include (i) Jet exit to plate distance (ii) Jet-to-Jet spacing (iii) Reynolds number. The parameters are investigated in 25 cases in different combinations of A_Z, Re, Xn

3.3 Data Reduction

Numerical results are obtained after solving the governing equations. The results are presented in non dimensional form. The dimensionless parameters appearing in the problem are Reynolds number, non dimensional pressure and Nusselt number. The jet Reynolds number is defined as follows

$$\mathrm{Re} = \frac{\rho V D}{\mu}$$

The non dimensional pressure is defined as the ratio of static pressure at particular location to the maximum static pressure

$$P^* = \frac{P}{P_{max}}$$

Heat transfer is presented in dimensionless form as Nusselt number

$$Nu = \frac{q_x D}{(T_{ip} - T_j)k}$$

4 .Results And Discussion

4.1 Line and Planes Considered for Results and Discussion

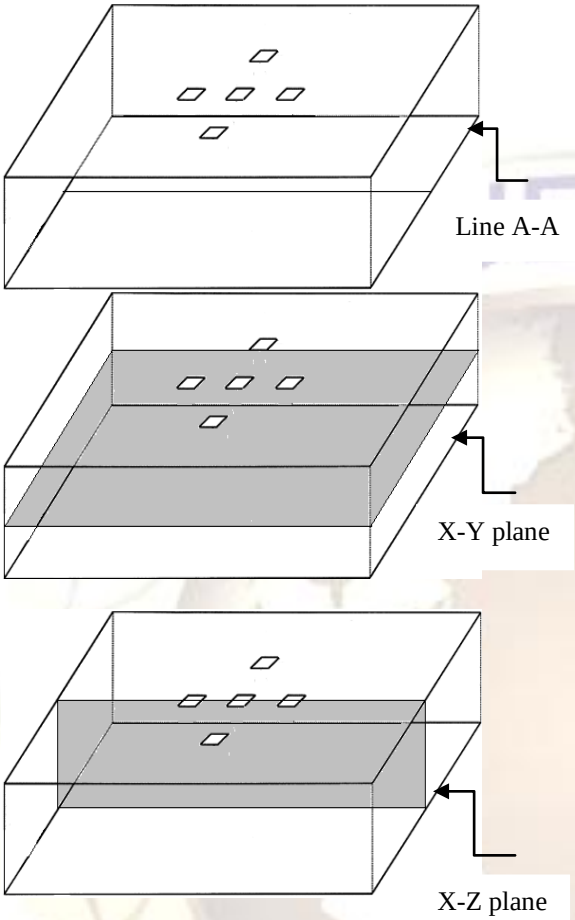

Fig.4 Line and Planes Considered for Results and Discussion

Line A-A which is shown in Fig.4 is considered to obtain the graphs for Nusselt number, Non dimensional pressure. Plane X-Y and Plane X-Z are considered to obtain contours of velocity, pressure.

4.2 Flow Structure Of Impinging Jets

As each of fluid jet eject out of the orifice with parabolic velocity profile a continuous reduction in velocity taken place from its center to the outer boundary .It is known that with increasing distance from exit and increasing momentum exchange between the jet and the ambient ,the free boundary of jet broadens while the potential core contacts on the impingement surface ,the wall jets are formed and spread radially. The wall jets emanating from each impinged form a collusion front due to interaction with neighbors. Consequently an up wash flow taken place. Thus overall structure consists of (1) potential core (2) shear layer (3) wall jets (4) up wash flow etc.

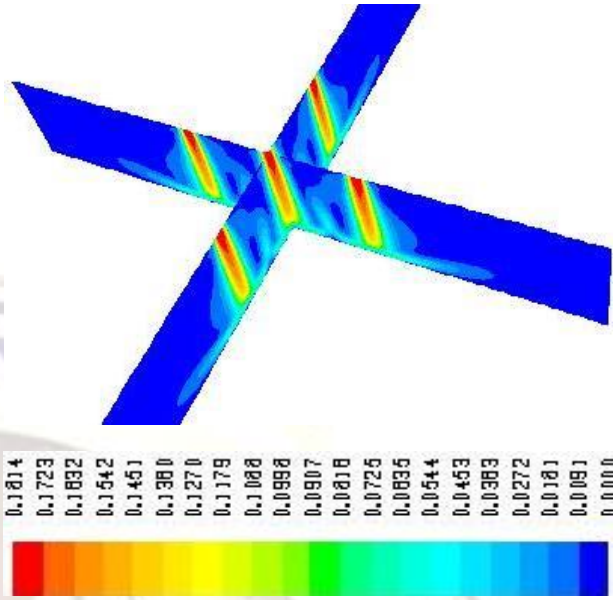

Fig.5 Velocity contours along XZ and YZ plane for Re=100, Xn=5D at A_Z=6

Figure 5 shows the velocity contour of five jets at A_Z=6 on XZ and YZ planes where vortices formed are clearly seen.

Figure 6 a-d shows the projection of flow lines on the mid vertical x–z plane for Re=100, X_n=5 and A_Z =1,2, 4, 6 and 8. For the rather small nozzle-to-plate spacing of 1 and 2 (Fig. 6 a and b) the up wash-fountain flows impinge on the top plate, forming wall jets at that plane. As the separation between the plates increases the up wash-fountain flows cannot reach the top plate, and as a result the upper wall jets cannot form (Fig. 6 c, d and e). The peripheral vortices stretch along the vertical direction and for A_Z =8 the peripheral vortex around the central jet is divided into two co-rotating vortices.

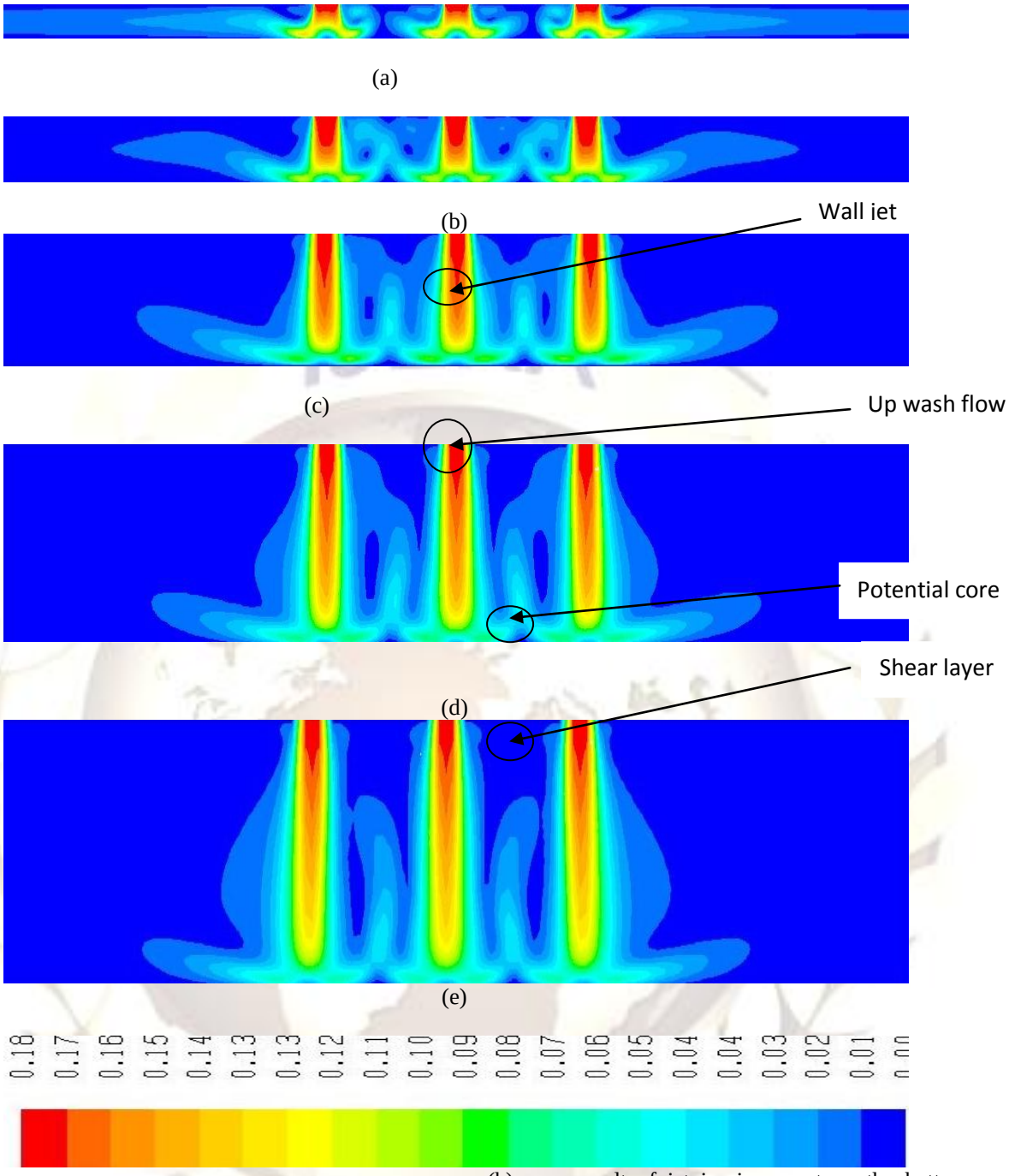

Fig. 6 Velocity contours for Re=100, X_n=5D and varying jet-to-plate distance
(a) A_Z =1, (b) A_Z =2 (c) A_Z =4 (d) A_Z =6 (e) A_Z=8.

The evolution of the entrainment vortex and wall jets is illustrated in Fig. 6 through a projection of the flow lines on different horizontal planes. Fig.7 (d) corresponds to a horizontal plane where upper wall jets are formed as up wash-fountains impinge on the top plate. The up wash-fountain flows are directed towards the jets near the top plate. The wall jet on the bottom plane starts forming at *Z*=-0.0016 Fig. 7 (b) as a result of jet impingement on the bottom plate. Further downstream, at *Z*=-0.0032, the wall jets are more prominent Fig. 7(a).

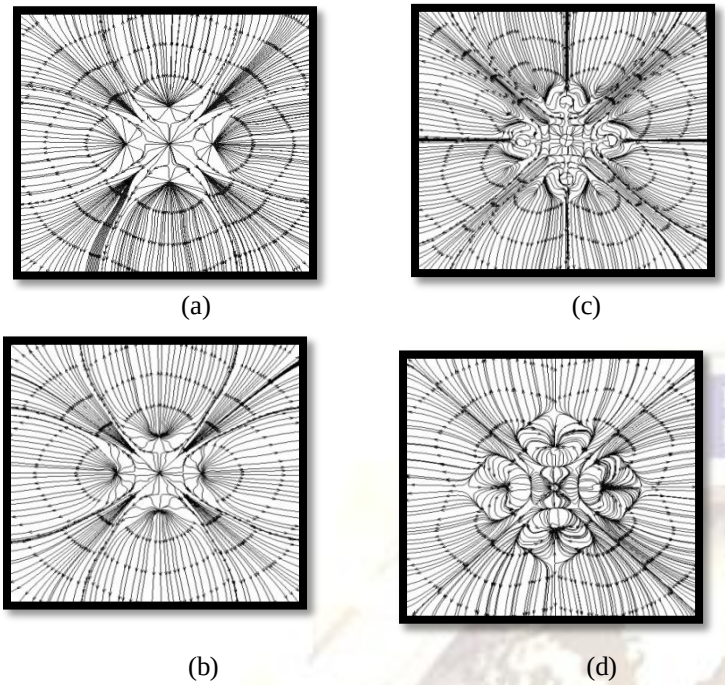

Fig.7 Projection of flow lines for Re=500, A_Z=1 and Xn=5D at horizontal cross-sections of (a) Z= -0.0032, (b) Z=-0.0016, (c) Z= 0 and (d) Z= 0.0032

The wall jet of the central jet spreads outward along the diagonal directions in between the wall jets, which are formed as the surrounding jets impinge on the bottom plate. The wall jets are separated from each other along the ground plane by stagnation lines or dividing lines everywhere between each impingement jet, containing a stagnation point.

The formation of the peripheral vortices and the wall jets for Re=300, Xn=5D is illustrated in Fig.8, using the projection of flow lines at different horizontal planes. The fluid is dragged radially towards the jets from the surrounding with complex flow patterns as shown in Fig. 8 (b–d). At elevations closer to the bottom plate, the flow pattern is characterized by the wall jets, which are separated from each other at the collision front (Fig. 8 a). The vertical component of the velocity of each jet has a single peak, which is located at the center of the jet.

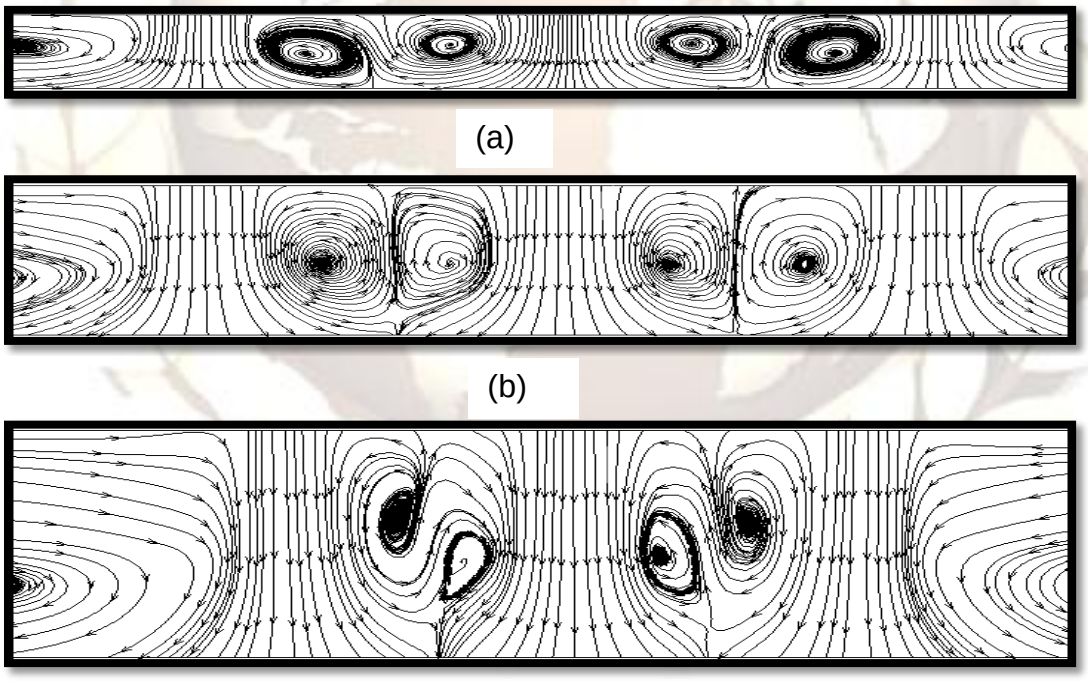

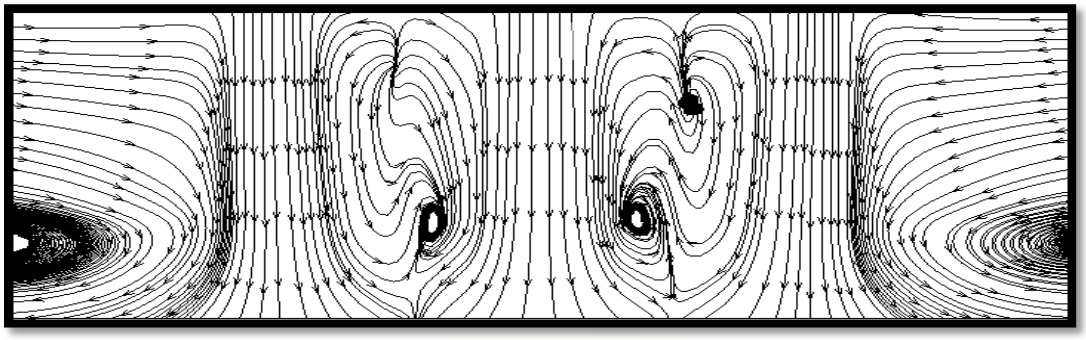

(d)

Fig. 8. Projection of flow lines on mid x-z plane for Re=100 and Xn=5D at jet-to-plate spacing (a) A_Z =2,
(b) A_Z =4, (c) A_Z =6 (d) A_Z =8.

4.3 Effect of Jet Exit to Plate Distance

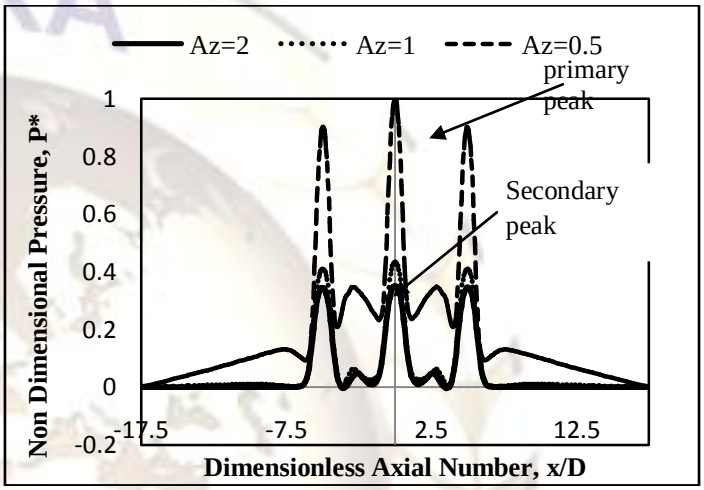

Fig.9 Non Dimensional Pressure for Re=300 Xn=5D by varying nozzle exit to plate distance along line A-A

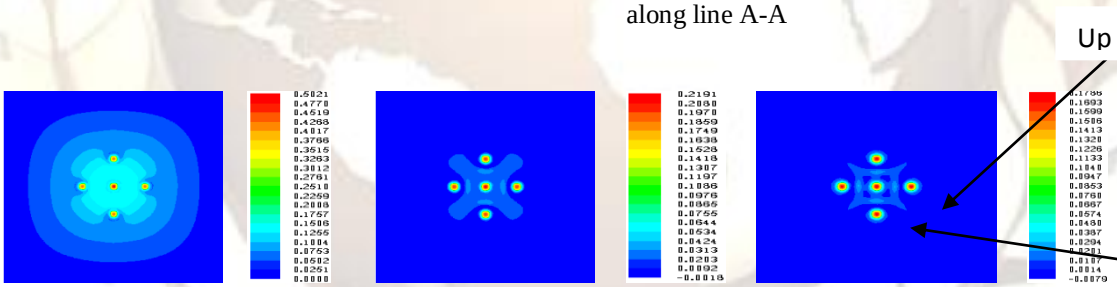

Fig.10 Pressure contours for Re=300, Xn=5D and varying A_Z value along XY plane (a) A_Z =0.5, (b) A_Z =1 and (c) A_Z =2.

Fig.9 shows the variation of non dimensional pressure distribution (P*) with different plate spacing to jet diameter ratio (A_Z) for Re (500) in line A-A. Peak pressure is observed at the point of stagnation of each jet .Jets are affected by zero momentum fluid (ambient air) hence the reduction of momentum in the free jet region is more than center jet. For AZ (1) and A_Z (2) the maximum pressure value in stagnation region is lower compared to pressure A_Z of 0.5. The lower value of pressure for higher A_Z may be attributed the entrainment of jet fountain fluid in the main jet.

This difference among the pressure values for different A_Z is smallest at the center jet compared to that at perimeter jets. This is because, the perimeter jets are more affected by quiescent ambient air. As discussed earlier the up wash fountain for lower A_Z is more prominent hence large peaks for lower A_Z values. Fig .10 shows the pressure contours for different A_Z values at Reynolds number 500.

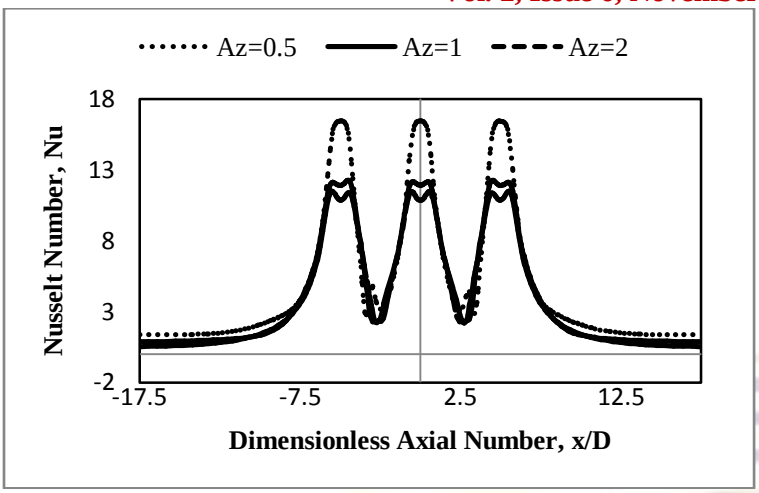

Fig.11 Nusselt number for Re=300, Xn=5D by varying jet to plate spacing along line A-A

Fig.11 shows the Nusselt number distribution along the stagnation line A-A for the case of A_Z =0.5, 1, 2. The trends of Nusselt number distribution from all jets are similar and symmetric about the stagnation point. However the exact values of the Nusselt number are not same for all the jets. With increase in A_Z values the Nusselt number decreases.

4.4 Effect of Reynolds Number

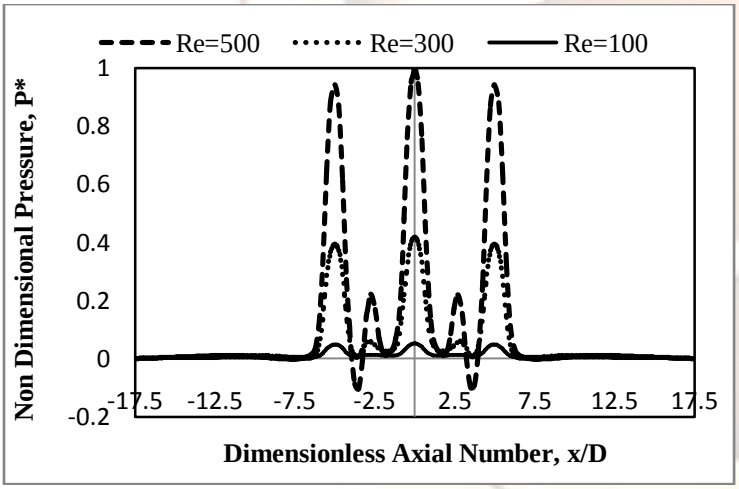

Fig.12 Non Dimensional Pressure for A_Z =1 Xn=5D by varying Reynolds number along line A-A

Figure12 shows dependence of dimensionless pressure distribution along line A-A on Reynolds number. As expected the Pressure peak is higher for high Reynolds number. At any Reynolds number the non dimensional pressure has the highest value at the stagnation region and reduces radially. Second peak is observed at the second stagnation point where neighboring wall jet collides.

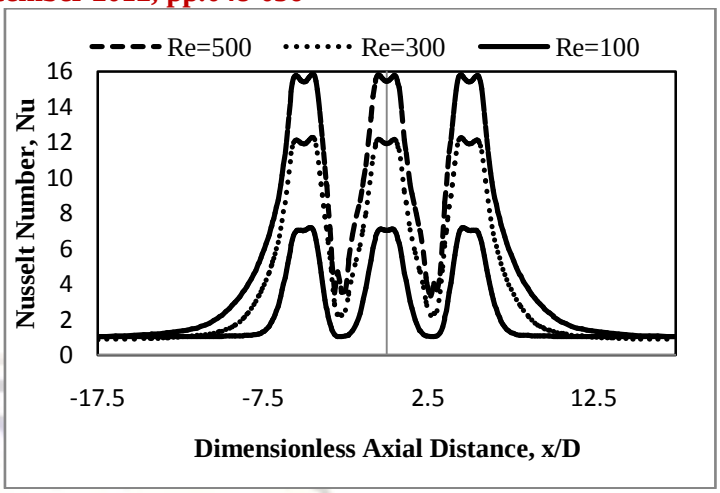

Fig: 13 Nusselt number for Xn=5d A_Z=1 by varying Reynolds number along line A-A

Position of secondary peak is independent of Reynolds number. The stagnation point pressure peaks for perimeter jets are smaller than center jets as they are affected by the quiescent ambient fluid. From Fig.13 it is clear that similar patterns were observed for Nusselt number i.e., with increase in Reynolds number Nusselt number also increases.

4.5 Effect of Jet to Jet Spacing

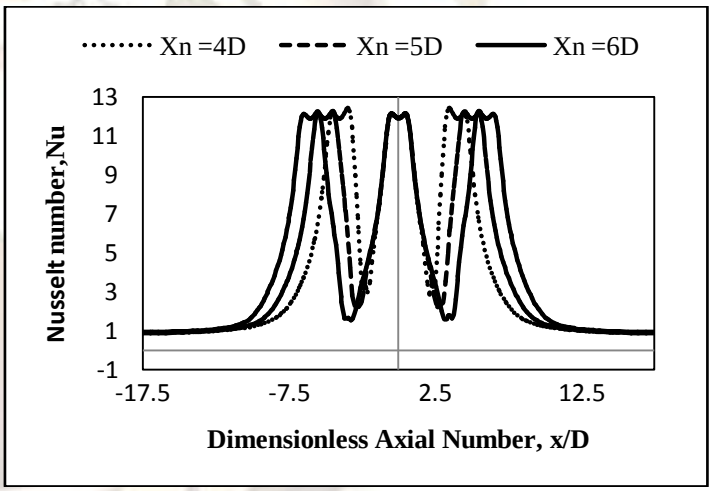

Fig.14 Nusselt Number for Re=300, A_Z =1 by varying jet-to-jet spacing along line A-A

The effect of jet-to-jet spacing, *Xn*, on the variation of local Nusselt number along *x*-direction at the mid- section is shown in Fig.13for *Re*=300and A_Z = 1. It is observed that the magnitude of the maximum Nusselt number is not affected by the jet-to-jet spacing.

Nomenclature

A_x, A_y, A_z - aspect ratios in x-, y- and z-direction, L_x/D, L_y/D, L_z/D
D - Jet width (m)
h - Heat transfer coefficient (W/m^2 K)
L_x, L_y, L_z - length of heated surface in x-, y- and z-directions respectively (m)
K - Thermal conductivity (W/m K)
Nu - local Nusselt number (hD/k)
P* - Non dimensional pressure (p/p_{max})
P - Static Pressure (N/m^2)
Pr - Prandtl number (ν/α)
q''_w - local convective heat flux at the impingement plate
Re - jet Reynolds number ($\frac{\rho VD}{\mu}$)
T - Non dimensional temperature, $(t-t_j)/(t_w-t_j)$
u_j - jet exit velocity (m/s)
U-Non dimensional Cartesian velocity, in x-direction (u/u_j)
V - Non dimensional Cartesian velocity, in y-direction (v/u_j)
W-Non dimensional Cartesian velocity, in z-direction (w/u_j)
u, v, w - Cartesian velocities
X_n, Y_n - jet-jet spacing in x- and y-directions, respectively
X, Y, Z - non dimensional Cartesian coordinates, x/D, y/D, z/D respectively
x, y, z - Cartesian coordinates

Greeks

ν - Kinematic viscosity (m^2/s)
ρ - Density (kg/m^3)
α - thermal diffusivity (m^2/s)
φ - U, V, W, P, or T field

Subscripts

J - jet exit
W - Wall

Conclusion

A three-dimensional numerical study is used to determine the flow and heat transfer characteristics of multiple impinging jets of square cross-section. The results indicate a rather complex flow field with the formation of a peripheral vortex around each jet and an up wash-fountain flow at the collision point of the jets. The size and location of any peripheral vortex depends on the nozzle-to-plate spacing. Moreover, the Nusselt number, far from the impingement zone is much higher than at larger nozzle-to-plate spacing due to higher wall jet velocities. In addition, no secondary peak of the Nusselt number was found for this small separation distance. Heat transfer is strongly affected by the jet-to-plate spacing. However, the magnitude of the maximum Nusselt number is not affected by the jet-to-jet spacing.

Reference

1. J. M. M. Barata, D. F. G. Durao, and M. V. Heitor, Impingement of Single and Twin Turbulent Jets through a Cross flow, *AIAA Journal*, vol. 29, no. 4, pp. 595-602, 1991.
2. A. R. P. V. Heiningen, A. S. Majumdar, and W. J. M. Douglas, Numerical Prediction of the Flow Field and Impinging Heat Transfer Caused by a Laminar Slot Jet, *ASME Journal of Heat Transfer*, vol. 98, pp. 654-658, 1976.
3. Y. J. Chou and Y. H. Hung, Impingement Cooling of an Isothermally Heated Surface with a Confined Slot Jet, *ASME Journal of Heat Transfer*, vol. 116, pp. 479-482, 1994.S. Mikhail, S. M. Morcos, M. M. M. Abou-Ellail, and W. S. Ghaly, Numerical Prediction of Flow Field and Heat Transfer from a Row of Laminar Slot Jets Impinging on a Flat Plat, *Proc. 7th Int. Heat Transfer Conf.*, vol. 3, pp. 337-382, 1982.
4. S. Mikhail, S. M. Morcos, M. M. M. Abou-Ellail, and W. S. Ghaly, Numerical Prediction of Flow Field and Heat Transfer from a Row of Laminar Slot Jets Impinging on a Flat Plat, *Proc. 7th Int. Heat Transfer Conf.*, vol. 3, pp. 337-382, 1982.
5. T. D. Yuan, J. A. Liburdy, and T. Wang, Buoyancy Effects on Laminar Impinging Jets, *Int. J. Heat Mass Transfer*, vol. 31, pp. 2137-2145, 1988
6. D. M. Schafer, F. P. Incropera, and S. Ramadhyani, Numerical Simulation of Laminar Convection Heat Transfer from an In-Line Array of Discrete Sources to a Confined Rectangular Jet, *Numeric. Heat Transfer, Part A*, vol. 22. pp. 121-141, 1992.
7. D. C. Wadsworth and I. Mudawar, Cooling of a Multichip Electronic Module by Means of Confined Two-Dimensional Jets of Dielectric Liquid, *ASME Journal of Heat Transfer*, vol. 112, pp. 891-898, 1990.
8. I. Sezai and A.A.Mohamad, 3-DSimulation of Laminar Rectangular Impinging Jets, Flow Structure and Heat Transfer, *ASME Journal of Heat Transfer*, vol. 121, pp. 50-56, 1999.
9. S. J. Slayzak, R. Viskanta, and F. P. Incropera, Effects of Interaction Between Adjacent Free Surface Planar Jets on Local Heat Transfer from the Impingement Surface, *Int. J.Heat Mass Transfer*, vol. 37, no. 2, pp. 269-282, 1994.
10. Clayton, D.J., and W. P. Jones**,** (2006) Large Eddy Simulation of Impinging Jets in a Confined Flow, *Flow Turbulence Combust*, 77: 127–146.
11. Jung-Yang and Mao-De (2001) investigated the effect of jet-to-jet spacing on the local Nusselt number for confined circular air jets vertically impinging on a flat plate.